

Polar Biosci., 19, 1–10, 2006
© 2006 National Institute of Polar Research

Estimation of the physical release of organic matter from ice using observational data and a coupled ice-water box model

Yoshiki Nishi^{1*} and Shigeru Tabeta²

¹Research Institute for Applied Mechanics, Kyushu University, 6-1, Kasuga-koen, Kasuga 816-8580

²Graduate School of Frontier Sciences, The University of Tokyo, 7-3-1, Hongo, Bunkyo-ku, Tokyo 113-0033

*Corresponding author. E-mail: nishiy@riam.kyushu-u.ac.jp

(Received March 28, 2005; Accepted June 15, 2005)

Abstract: In order to estimate the physical release of organic matter from sea ice and biological production in the ice, we conducted a series of field observations (samplings of water beneath the ice and of an ice core, and deployment of sediment traps) on the ice on Saroma Ko lagoon, Hokkaido, Japan in 2004 and developed a coupled ice-water box model. The observations documented the accumulation of organic matter in the ice. The box model estimates biological production in the ice at $208 \text{ mgC m}^{-2} \text{ day}^{-1}$ (Mar. 1–2) and $60 \text{ mgC m}^{-2} \text{ day}^{-1}$ (Mar. 2–11), and estimates the fluxes of the physical release at $142 \text{ mgC m}^{-2} \text{ day}^{-1}$ (Mar. 1–2) and $68 \text{ mgC m}^{-2} \text{ day}^{-1}$ (Mar. 2–11), which account for more than 70% of biological production in the ice. The physical release efficiently transports organic matter from sea ices to water column.

key words: ice algae, release, box model, production, Saroma

Introduction

Ice algae are known to have an important role in primary production in high latitude oceans (e.g. Legendre *et al.*, 1992; Gosselin *et al.*, 1997). Most of the ice algae are released from ice. For instance, Garrison and Buck (1985) demonstrated that the same species are usually found in both sea ice and water in the Weddell Sea in the Antarctic, and suggested that an ice-edge bloom is seeded by algae released from the ice. Furthermore, Runge and Ingram (1991) reported that released algae are actively grazed by copepods in southeastern Hudson Bay. On the other hand, Riebesell *et al.* (1991) demonstrated that since algal cells form aggregates after their release, they rapidly sink.

Additional estimates of the ice algal release have been made by some previous studies; Smith *et al.* (1988), McMinn (1996), and Michel *et al.* (1996). These studies estimated the amount of released organic matter by comparing the observed biomass of POC in ice with one predicted by using an experimental equation representing ice-algal growth. However, there are some problems in the generality of the method employed and in the dependence on some of the parameters in the equation. Thus, in these previous studies, the material cycle in ice-covered seas has not been quantitatively estimated. In order to clarify the mechanism of the material cycle, the release of mat-

ter from ice needs to be adequately estimated.

A coupled ice-ocean ecosystem model developed by Nishi and Tabeta (2005) made it possible to calculate the coupling processes between ice and water. They conducted numerical simulations using this model and showed that the mechanisms of release are compound effects of dynamics (diffusion at ice bottom), thermodynamics (ice-melting) and glaciology (brine convection). From this conclusion, they called the release of organic matter the “physical releasing effect”. Estimation of the release flux by observation-based methods is useful for the observational studies of material cycle in ice-covered sea, and is indispensable to validation of the numerical model (Nishi and Tabeta, 2004).

Therefore, in this study, a field observation has been conducted, and a coupled ice-water box model using observational data, which is able to estimate biological production in ice and release flux from ice, is developed and used.

Materials and methods

Field observation

An *in-situ* study was conducted on the sea ice on Saroma Ko lagoon, Hokkaido, Japan from Feb. 26 to Mar. 11, 2004. The location and topography of the lagoon ($44^{\circ}07'N$, $143^{\circ}57'E$) is shown in Fig. 1. Saroma Ko lagoon is a large body of brackish water separated from the ocean (the Sea of Okhotsk) by a narrow sandbar. Water exchange through two inlets (1st and 2nd inlets) is driven mainly by diurnal tides. This lagoon is located in the southernmost sea ice-covered region in the northern hemisphere, and is a useful field site because the calm condition of the lagoon ensures that the ice persists through winter.

Three types of samples were collected: ice cores, water beneath the ice, and sinking matter. Ice cores were collected with an ice auger. The bottom 0.1 m portions of the

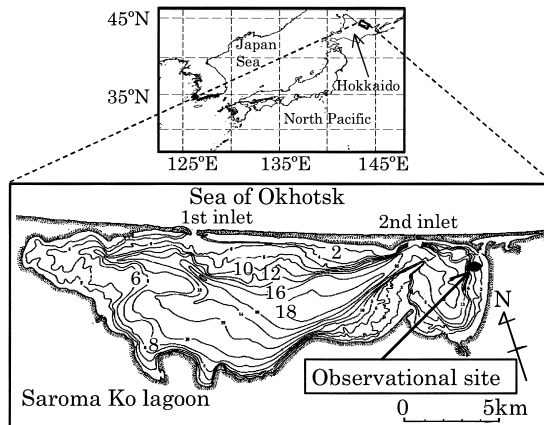


Fig. 1. Upper panel: The location of Saroma Ko lagoon. Lower panel: The topography in Saroma Ko lagoon. Contour lines represent water depths (m). The closed circle denotes the observational site from February 26 to March 11, 2004.

Table 1. Summary of sampling methods, measured items and sampling date.

Sampling method	Measured items	Sampling date
Water	Chl. <i>a</i> , POC, PON, and nutrients	Feb. 26, 27, Mar. 1, 2, and 11
Ice core	Same as water	Same as water
Sediment trap	Chl. <i>a</i> , POC, and PON	Feb. 26–28, Mar. 1–2, and Mar. 2–11

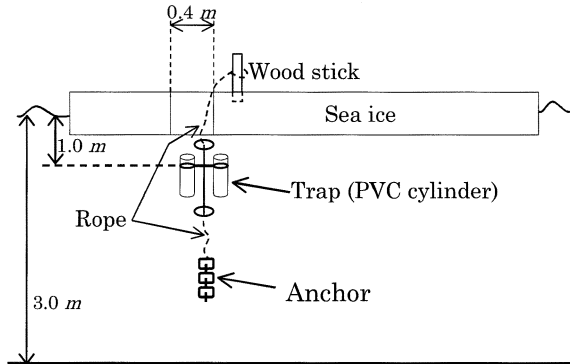


Fig. 2. A schematic drawing of the method of sediment trap deployment.

core, which corresponds to the layer that most of the ice algae inhabited, were cut and put in artificial sea water (35.0 psu) in cool dark conditions for melting. Water beneath the ice, at a depth of 1.0 m below the water surface, was sampled using a Niskin bottle. The sampling dates of the ice and water are listed in Table 1. Sinking matter beneath the ice was collected by sediment traps, which were deployed at a depth of 1.0 m below the water surface during the three periods described in Table 1. The traps used in this observation were made of polyvinyl chloride (PVC) circular cylinders with a diameter of 75.0 mm and with an aspect ratio (height/diameter) of 3.0. This ratio is known to be suitable for effective collecting of sinking matter in sea water (S. Taguchi, pers. commun.). The schematic drawing of the deployment is shown in Fig. 2. Two traps were connected at the same depth in order to obtain duplicate samples. First, the traps were deployed by cutting a square hole with a width of 0.40 m through the ice. Next, the traps, which had been previously filled with artificial sea water (salinity was 35.0 psu), were placed in the water under the hole. After mooring the traps, the removed piece of sea ice was returned to its original place. When the traps were pulled up, water in the traps was poured into a plastic package, and was kept in a cool and dark place.

The collected samples were transported to a laboratory near the observational site and were divided into four sub-samples by using a sample splitter. Pressure filtration was undertaken on all of the sub-samples. Other samples were filtrated in duplicate through $0.45\ \mu\text{m}$ -mesh filters and the filtrates were kept frozen for nutrient analysis (NO_3 , NO_2 , PO_4 , and SiO_2) using an auto-analyzer (Bran-Luebbe AACS-II). Two sub-samples were filtered onto Whatman GF/F glass-fiber filters, which were soaked in DMF (*n,n*-Dimethylformamide) poured in dark vial containers for the extraction of chlorophyll *a*. The extracted solutions were processed in a Turner Design Fluorometer

Model (10AU) in order to measure chlorophyll *a* concentration fluorometrically (Holm-Hansen *et al.*, 1965). Two other sub-samples were filtered onto pre-combusted (500°C, 2 hours) Whatman GF/F glass-fiber filters, and were kept in the cool and dark condition. After drying (60°C, 24 hours), the POC and PON in the filters were measured using a CHN coder (FISONS INSTRUMENTS).

Box model

In this study, we propose a simple method for estimating production in ice and release from ice without using biological parameters. A box model based on data obtained from the field observation was constructed. The model considers two boxes: an ice box and a water box. The ice and water box have a thickness of the ice layer inhabited by ice algae: $h_i = 0.1$ m and of the water layer $h_w = 1.0$ m which is equivalent to the depth of trap deployment. A schematic view of the box model is drawn as Fig. 3. The mass flux of organic carbon released from ice is calculated by solving simultaneous algebraic equations. Equations (1) and (2) describe the carbon budget in the ice and water boxes, respectively;

$$\underbrace{h_i \frac{\partial C_i}{\partial t}}_{(A)} = \underbrace{(\text{Net production})}_{(B)} - \underbrace{(\text{Physical release})}_{(C)}, \quad (1)$$

$$\underbrace{h_w \frac{\partial C_w}{\partial t}}_{(D)} = \underbrace{(\text{Physical release})}_{(E)} - \underbrace{(\text{Export})}_{(F)}, \quad (2)$$

where t represents time, and C_i and C_w denote the concentrations of POC in ice and in water, respectively. There are two assumptions in the above formulation. First, horizontal transport of organic carbon in water and in ice is ignored because the speed

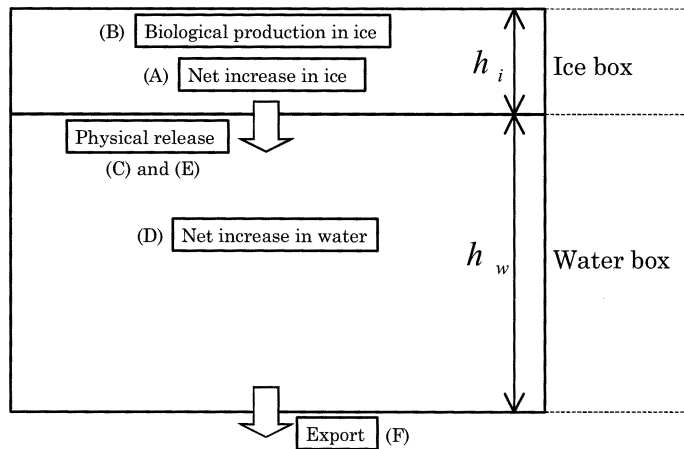


Fig. 3. A schematic view of the coupled ice-water system considered in the box model. Letters (A, B, C, D, E, and F) correspond to the terms in eqs. (1) and (2).

of water flow under the ice at the observational site was less than a few centimeters per second and because the drift of ice in Saroma Ko lagoon is negligibly small (Takeuchi *et al.*, 1990). Second, biological production in the water box is ignored because the primary production by pelagic phytoplankton during winter is much lower than that by ice algae in Saroma Ko lagoon (Hattori *et al.*, 2001).

There are six terms in the formulation of the box model. (A) and (D) represent the net increase of organic carbon in the ice box and in the water box, respectively. (B) represents biological production in the ice box. (C) and (E) denote the flux of organic carbon released from the ice. (F) represents the flux of the export of POC which equals the sinking flux at the bottom of the water box. Among them, (A) and (D) are calculated directly by substituting the observed concentrations of POC. (F) is estimated using the POC sinking flux obtained from the sediment trap. Since (C) is equivalent to (E), there are two unknown terms, (B) and (C=E), which are computed by solving the equations. The carbon budgets were estimated for Mar. 1–2 and Mar. 2–11, 2004.

Results

Biomass in ice and in water

Figure 4a shows temporal variations in the standing stock of chlorophyll *a* in ice (depicted as \blacklozenge), and in water (depicted as \circ). Chlorophyll *a* in the ice rapidly

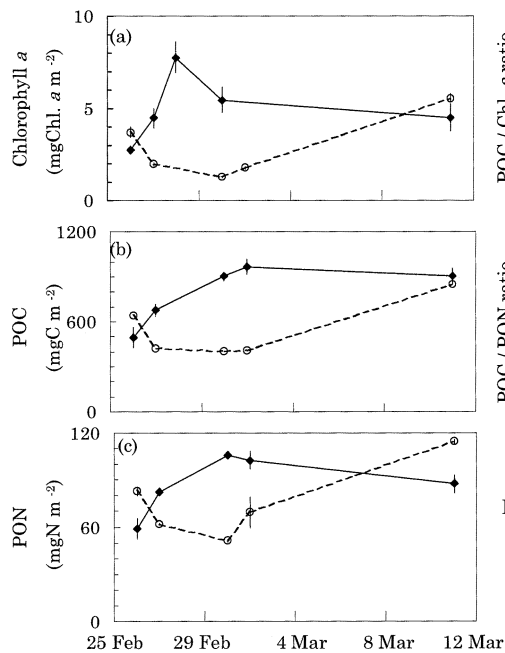


Fig. 4. Temporal variations in the standing stocks of (a) chlorophyll *a*, (b) POC, and (c) PON in ice (\blacklozenge), and in water (\circ). The vertical bars denote standard deviations.

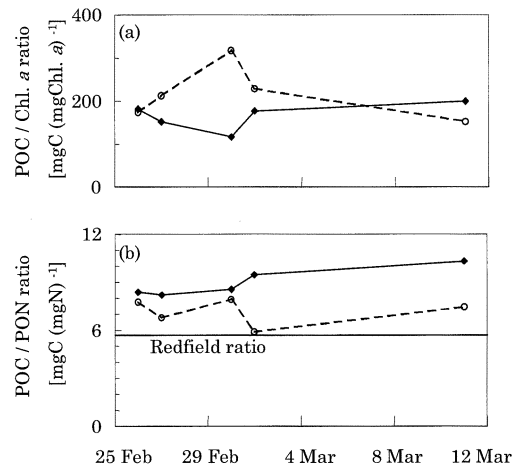


Fig. 5. Temporal variations in the weight ratios of (a) POC to chlorophyll *a*, and of (b) POC to PON in ice (\blacklozenge), and in water (\circ).

increased in late February. Conversely, chlorophyll *a* in the water during this period decreased. In March, chlorophyll *a* in the ice decreased while that in the water increased. Figure 4b shows temporal variations in the standing stock of POC in the ice (\blacklozenge), and in the water (\circ). POC in the ice rapidly increased in late February and decreased in March. POC in the water decreased in the late February and increased in March. Hence, patterns of the variations in POC were mostly in parallel with those in chlorophyll *a*. The standing stock of PON shown in Fig. 4c also had variations similar to those of chlorophyll *a* and POC.

POC/Chl. *a* ratio and POC/PON ratio

Figure 5 shows the temporal variations of (a) POC/Chl. *a*, and (b) POC/PON ratios (by weight) in ice (\blacklozenge), and in water (\circ). The POC/Chl. *a* ratio in the ice ranges from 116 to 200 with an average value of 165. The POC/Chl. *a* ratio in the water ranges from 153 to 317 with an average value of 217. The POC/PON ratios in the ice and in the water are higher than the Redfield ratio.

Nutrient concentrations in ice and in water

Concentrations of nutrients in ice (\blacklozenge), and in water (\circ) are shown in Fig. 6: (a) nitrate, (b) nitrite, (c) silicate, and (d) phosphate. The concentrations of nitrate, nitrite, silicate, and phosphate in the water had a range from 5 to $15\mu\text{mol l}^{-1}$, from 0.2 to $0.5\mu\text{mol l}^{-1}$, from 40 to $120\mu\text{mol l}^{-1}$, and from 0.3 to $0.5\mu\text{mol l}^{-1}$, respectively.

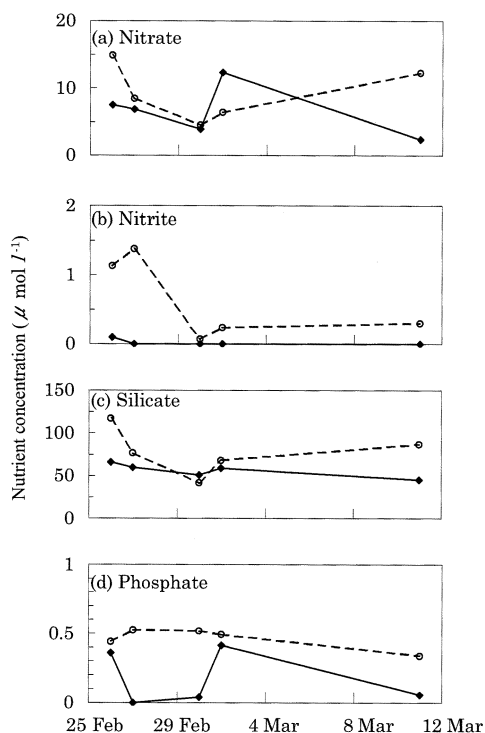


Fig. 6. Time histories of nutrient concentrations in ice (\blacklozenge), and in water (\circ): (a) nitrate (NO_3), (b) nitrite (NO_2), (c) silicate (SiO_2), and (d) phosphate (PO_4).

Most of the nutrient concentrations in the ice had lower values than those in the water. On average, ratios of concentrations in ice to those in water are as follows: nitrate: 0.71, nitrite: 0.03, silicate: 0.71, and phosphate: 0.37.

Sinking flux

Sinking fluxes of (a) POC and (b) chlorophyll *a* are shown in Fig. 7. The POC sinking flux increased from the end of February (Feb. 26–28) to the beginning of March (Mar. 1–2). The POC sinking flux from Mar. 2 to Mar. 11 was the smallest among the observed fluxes. Time variations in the chlorophyll *a* sinking flux were similar to those in the POC sinking flux. A scatter diagram of the two sinking fluxes is shown in Fig. 8. An examination of the relationship between the two sinking fluxes revealed a high correlation between them ($R^2=0.9936$). The POC/Chl. *a* ratios of the sinking flux for

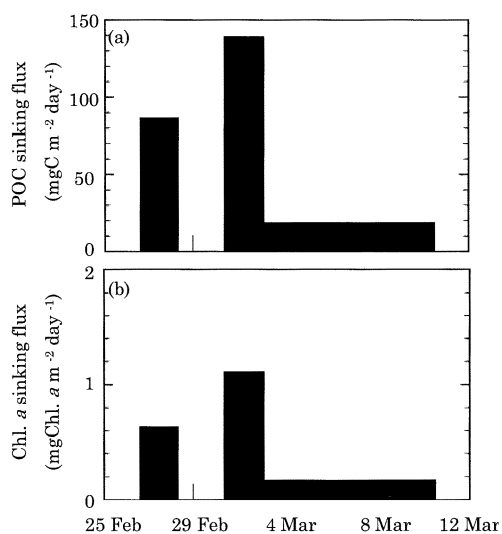


Fig. 7. Time variations in the sinking flux of (a) POC, and (b) chlorophyll *a* at depth 1.0 m measured with sediment traps.

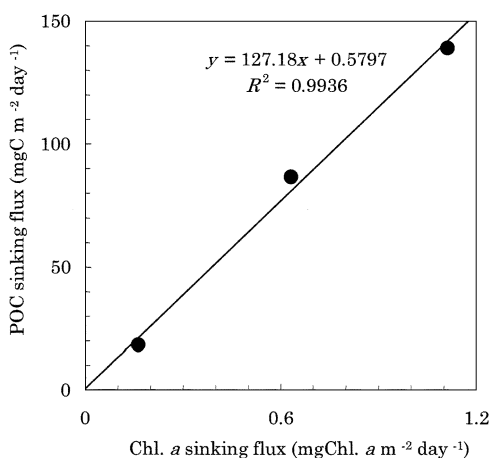


Fig. 8. Scatter plots of the sinking flux of chlorophyll *a* versus that of POC. The solid line has been calculated by the least-square method.

Table 2. Estimation method of each term in the governing equations of the box model (1) and (2) and the results of the estimation. All calculated values have the unit of $\text{mgC m}^{-2} \text{day}^{-1}$.

Term in the eqs. (1), (2)	Estimation method	Mar. 1–2	Mar. 2–11
(A)	Observed	66.24	−7.34
(B)	Calculated by eq. (1)	208.21	60.34
(C)	Same as (E)	141.97	67.68
(D)	Observed	2.84	49.20
(E)	Calculated by eq. (2)	141.97	67.68
(F)	Observed	139.13	18.48

the three deployment periods were 137 (Feb. 26–28), 125 (Mar. 1–2), and 113 (Mar. 2–11) with an average of 125.

Carbon fluxes in a coupled ice-water system

The results obtained from the box model are presented in Table 2. The calculated biological production in the ice (term (B)) decreased from Mar. 1–2 ($208 \text{ mgC m}^{-2} \text{ day}^{-1}$) to Mar. 2–11 ($60 \text{ mgC m}^{-2} \text{ day}^{-1}$). This change is influenced mainly by the decreasing trend of the POC concentrations in ice observed from Mar. 2 to 11 shown in Fig. 4. The estimated flux of physical release from ice (term (C) or (E)) also had a decreasing trend from Mar. 1–2 ($142 \text{ mgC m}^{-2} \text{ day}^{-1}$) to Mar. 2–11 ($68 \text{ mgC m}^{-2} \text{ day}^{-1}$). Comparison of term (C) (or (E)) with term (B) showed that the physical release accounts for 68% (Mar. 1–2) and 112% (Mar. 2–11) of the biological production.

Discussion

The nitrate and nitrite concentrations in the water (1.0 m depth) observed in 2004 are similar to those observed in 1992 by Taguchi *et al.* (1994); nitrate: $5\text{--}15 \mu\text{mol l}^{-1}$ and nitrite: $0.2\text{--}0.5 \mu\text{mol l}^{-1}$. The silicate concentrations in the water (1.0 m depth) observed in 2004 are higher than those observed in 1992 by Taguchi *et al.* (1994); $10\text{--}30 \mu\text{mol l}^{-1}$. In contrast, phosphate concentrations in the water (1.0 m depth) observed in 2004 are lower than those observed in 1992 by Taguchi *et al.* (1994); $0.3\text{--}1.3 \mu\text{mol l}^{-1}$. The result that the concentrations of the nutrients in ice were mostly lower than those in water, reflects following two phenomena: first, consumption of nutrients by photosynthetic activity of ice algae, and second, brine rejection during ice freezing.

The qualitative pattern of chlorophyll *a* variation in the ice (Fig. 4a) is similar to that observed in 1992 by Kudoh *et al.* (1997), who also observed a variation of chlorophyll *a* in ice that increased in late February and decreased in early March. The increasing variations of POC and PON in parallel with that of chlorophyll *a* in the ice (Fig. 4) demonstrates that ice algae had grown, and that organic matter had accumulated in the ice. The standing stocks in the ice in 2004 are lower than those in 1992 reported by Kudoh *et al.* (1997). One reason is probably the later advance of the sea ice in Saroma Ko lagoon in 2004 as described by McMinin *et al.* (2005). The biological production calculated by the box model is approximately consistent with that ($54.1\text{--}343.2 \text{ mgC m}^{-2} \text{ day}^{-1}$) by Hattori *et al.* (2001), who estimated the primary production of ice algae at Saroma Ko lagoon using the ^{13}C method. The sinking fluxes (1.0 m depth) of chlorophyll *a* and of POC obtained from the present study approximately correspond to those (0.5 m depth) observed in 1992 by Michel *et al.* (1997). The average of POC/Chl. *a* ratios in the ice and in the water is higher than that of ice algae (7.2–23.3) measured by Kudoh *et al.* (1997). The reasons for this are as follows: first, POC concentrations measured in this study include also the organic matter besides the ice algae. Second, the light intensity inside the ice during the period of ice algal growth in 2004 could have been higher than in previous years because of the later and thinner ice condition in Saroma Ko lagoon in 2004. The POC/Chl. *a* ratio of ice algae generally becomes higher (lower) as daily-integrated PAR increases (decreases) due to

ice algal light/shade adaptation states (Arrigo and Sullivan, 1994). Besides, the lower POC/Chl. *a* ratio of the sinking flux than that in the water suggests that the relative contribution of the released algae to the sinking flux is higher than to the suspended matter. This is because of the high sinking speed of the released algae (Riebesell *et al.*, 1991).

The results obtained from the box model show that the flux of physical release from the ice accounts for 68–112% of the biological production in the ice. This means that the organic matter produced in the ice is efficiently transported into the water beneath the ice. Therefore, the box model analysis quantitatively showed the importance of the release in the material transport in the ice-covered ecosystem. In addition, the correlation between sinking fluxes of POC and chlorophyll *a* in Fig. 8 suggests that the sinking matter was composed mostly of matter that had contained chlorophyll *a*. If sinking matter had included many components that did not contain chlorophyll *a*, the *y*-intercept of the regression line in Fig. 8 would have shifted to a non-zero position. From these results, most of the sinking matter beneath the ice (1.0 m depth) were composed of living ice algae, which had been released from the ice through the physical releasing effect that is driven by ice-melting, diffusion on the bottom of the ice, and brine convection.

In the present study, a few assumptions are imposed for the simplicity of the box model formulation. The second assumption (minimal production by pelagic phytoplankton) is not always valid: for example, McMinn *et al.* (2005) recently reported that relative contribution of the ice algae and of the phytoplankton to total gross photosynthesis in Saroma Ko lagoon are 54.3% and 32.6%, respectively. In addition, several kinds of grazers (*e.g.* copepods and mysids), which harvest ice algae at the bottom of the sea ice and released algae beneath the sea ice (*e.g.* Runge and Ingram, 1991) might considerably contribute the net production in pelagic system as secondary producers. Furthermore, natural losses of biological production (lysis of bacteria, fungi, and virus) in the pelagic system also exist in the real ecosystem. Therefore, for more accurate estimation, it is necessary to develop a renewed box model that includes also net production in the pelagic system as a variable. An idea to achieve this is to determine the release flux as not an induced variable but as an independent variable by measurements that utilize traps moored at a closer depth to the undersurface of the sea ice.

The traps were deployed only a few times due to logistic problems in this study. The use of a multiple sediment trap (*e.g.* Taguchi *et al.*, 1997) could make it possible to estimate the release flux more continuously using the proposed box model.

Acknowledgments

The authors would like to thank Drs. S. Taguchi, H. Hattori, and N. Ohi for help in the field and laboratory, and for their useful comments. We are grateful to Drs. K. Shirasawa, T. Kawamura, M. Ishikawa, T. Takatsuka, K. Tateyama, and S. Uto for help in the field work. The design and production of the sediment traps by Mr. T. Kato is greatly acknowledged. All laboratory measurements were conducted by using the apparatus of Dr. S. Taguchi's laboratory, Soka University.

References

- Arrigo, K.R. and Sullivan, C.W. (1994): A high resolution bio-optical model of microalgal growth: Tests using sea ice algal community time-series data. *Limnol. Oceanogr.*, **39**, 609–631.
- Garrison, D.L. and Buck, K.R. (1985): Sea-ice algal communities in the Weddell Sea: species composition in ice and plankton assemblages. *Marine Biology of Polar Regions and Effects of Stress on Marine Organisms*, ed. by J.S. Gray and M.E. Christiansen. New York, John Wiley, 103–122.
- Gosselin, M., Levasseur, M., Wheeler, P.A., Horner, R.A. and Booth, B.C. (1997): New measurement of phytoplankton and ice algal production in the Arctic Ocean. *Deep-Sea Res.*, **44**, 1623–1644.
- Hattori, H., Kato, C. and Saito, H. (2001): Seasonal change in primary production in Saroma-ko, subarctic lagoon, eastern Hokkaido. *Proc. 16th International Symp. Okhotsk Sea & Sea Ice*, 66–69.
- Holm-Hansen, O., Lorenzen, C.J., Holmes, R.N. and Strickland, J.D.H. (1965): Fluorescence determination of chlorophyll. *J. Cons. Perm. Int. Explor. Mer.*, **30**, 3–15.
- Kudoh, S., Robineau, B., Suzuki, Y., Fujiyoshi, Y. and Takahashi, M. (1997): Photosynthetic acclimation and the estimation of temperate ice algal primary production in Saroma-ko Lagoon, Japan. *J. Mar. Syst.*, **11**, 93–109.
- Legendre, L., Ackley, S.F., Dieckmann, G.S., Gulliksen, B., Horner, R., Hoshiai, T., Melnikov, I.A., Reeburgh, W.S., Spindler, M. and Sullivan, C.W. (1992): Ecology of sea ice biota 2. Global significance. *Polar Biol.*, **12**, 429–444.
- McMinn, A. (1996): Preliminary investigation of the contribution of fast-ice algae to the spring phytoplankton bloom in Ellis Fjord, eastern Antarctica. *Polar Biol.*, **16**, 301–307.
- McMinn, A., Hirawake, T., Hamaoka, T., Hattori, H. and Fukuchi, M. (2005): Contribution of benthic microalgae to ice covered coastal ecosystem in northern Hokkaido, Japan. *J. Mar. Biol. Ass. U.K.*, **85**, 283–289.
- Michel, C., Legendre, L., Ingram, R.G., Gosselin, M. and Levasseur, M. (1996): Carbon budget of sea-ice algae in spring: Evidence of a significant transfer to zooplankton grazers. *J. Geophys. Res.*, **101**, 18345–18360.
- Michel, C., Legendre, L. and Taguchi, S. (1997): Coexistence of microalgal sedimentation and water column recycling in a seasonally ice-covered ecosystem (Saroma-ko, Lagoon, Sea of Okhotsk, Japan). *J. Mar. Syst.*, **11**, 133–148.
- Nishi, Y. and Tabeta, S. (2004): Observation and modeling for ice-ocean coupled ecosystem in the coastal lagoon, Saroma-ko. *Proc. 04MTS/IEEE/TECNO-OCEAN'04 (OTO'04)*, 1649–1654.
- Nishi, Y. and Tabeta, S. (2005): Analysis of the contribution of ice algae to the ice-covered ecosystem in Saroma Ko lagoon by means of a coupled ice-ocean ecosystem model. *J. Mar. Syst.*, **55**, 249–270.
- Riebesell, U., Scholoss, I. and Smetacek, V. (1991): Aggregation of algae released from melting sea ice: implications for seeding and sedimentation. *Polar Biol.*, **11**, 239–248.
- Runge, J.A. and Ingram, R.G. (1991): Under-ice feeding and diel migration by the planktonic copepods *Calanus glacialis* and *Pseudocalanus minutus* in relation to the ice algal production cycle in southeastern Hudson Bay, Canada. *Mar. Biol.*, **108**, 217–225.
- Smith, R.E.H., Anning, J., Clement, P. and Cota, G. (1988): Abundance and production of ice algae in Resolute Passage, Canadian Arctic. *Mar. Ecol. Prog. Ser.*, **48**, 251–263.
- Taguchi, S., Demers, S., Fortier, L., Fortier, M., Fujiyoshi, Y., Hattori, H., Kasai, H., Kishino, M., Kudoh, S., Legendre, L., Mcginess, F., Michel, C., Ngando, T., Robineau, B., Suzuki, Y., Takahashi, M., Therraiault, J.C., Aota, M., Ikeda, M., Ishikawa, M., Takatsuka, T. and Shirasawa, K. (1994): Biological data report for Saroma-ko site of the SARES (Saroma-Resolute Studies) Project, February–March, 1992. *Low Temp. Sci. Ser. A Data Rep.*, **53**, 67–163.
- Taguchi, S., Saito, H., Hattori, H. and Shirasawa, K. (1997): Vertical flux of ice algal cells during the ice melting and breaking periods in Saroma ko Lagoon, Hokkaido, Japan. *Proc. NIPR Symp. Polar Biol.*, **10**, 56–65.
- Takeuchi, T., Sakata, T. and Hayase, Y. (1990): A study of the environmental conservation in lagoons of cold regions. *Rep. Civil Eng. Res. Inst.*, **92**, 1–103 (in Japanese).